Inhibition Effect of Rhodanine-N-Acetic Acid on Copper Corrosion in Acidic Media

ARTICLE *in* INDUSTRIAL & ENGINEERING CHEMISTRY RESEARCH · JULY 2013

Impact Factor: 2.59 · DOI: 10.1021/ie400160x

3 AUTHORS, INCLUDING:

Ayşe Ongun Yüce
Cukurova University
7 PUBLICATIONS **172** CITATIONS
SEE PROFILE

Gülfeza Kardaş
Cukurova University
62 PUBLICATIONS **1,887** CITATIONS
SEE PROFILE

I&EC research
Industrial & Engineering Chemistry Research

Article

pubs.acs.org/IECR

Inhibition Effect of Rhodanine-N-Acetic Acid on Copper Corrosion in Acidic Media

Ali Döner,* Ayşe Ongun Yüce, and Gülfeza Kardaş

Chemistry Department, Science and Letters Faculty, Çukurova University, 01330 Adana, Turkey

ABSTRACT: The inhibition effect of Rhodanine-N-acetic acid (R-NA) on copper corrosion in acidic media is studied by using potentiodynamic polarization, electrochemical impedance spectroscopy (EIS), and linear polarization resistance (LPR). The surface morphology is investigated by using scanning electron microscopy (SEM). The exposure of copper surface to 0.5 M H_2SO_4 solution in short and long immersion times in the absence and presence of the inhibitor is also examined. The results show that R-NA is a powerful inhibitor for copper corrosion in acidic media due to its strong adsorption onto the metal surface. Moreover our results are compared with similar compounds in the literature.

1. INTRODUCTION

Copper is an important material in industry due to its high electric and thermal conductivities, mechanical workability, and its relatively noble properties. It is widely used in many applications in electronic industries and communications as a conductor in electric power lines, domestic pipelines for and material in heating and cooling systems.[1] Although it has widespread applications, its poor resistance to corrosion is a major problem. For example, this can cause the heating and cooling systems to decrease in heating efficiency. These systems are cleaned by acid-pickling processes to reduce these negative effects (using sulfuric or hydrochloric acid). During the acid-pickling processes, copper does not displace hydrogen from acid solutions, but the presence of dissolved O_2 is responsible for its dissolution.[2] Therefore, many organic compounds are used to inhibit copper corrosion during these applications in recent years.

The use of organic compounds effectively eliminates the undesirable destructive effect and prevents metal dissolution.[3] The inhibition effect of organic compounds is usually attributed to their interactions with the copper surface via their adsorption. It is observed that the effective compounds for this area are the ones containing polar groups, including nitrogen, sulfur, and oxygen,[4−11] and heterocyclic compounds with polar functional groups and organic compounds possessing conjugated double bonds.[12−15] Polar functional groups are regarded as the reaction center that stabilizes the adsorption process.[16] In addition, it is well-known that the adsorption of an inhibitor on a metal surface depends on the chemical nature of the surface charge of metal, adsorption mode, and the type of the electrolyte solution.[17] The R-NA molecule has an additional acetic acid group which is assumed to be an active center of the adsorption, and it contributes to the solubility of the molecule in aqueous media. Therefore, the molecule is expected to show good adsorption ability and corrosion inhibition efficiency. R-NA and rhodanine were found to be good corrosion inhibitors for mild steel[18−21] and stainless steel.[22] Rhodanine derivates previously polymerized and found that this polymer provided a good protection for copper in H_2SO_4 solution.[23] R-NA and its analogs are also known to possess anticonvulsant,[24] antibacterial,[25] antiviral,[26] and antidiabetic activities.[27] R-NA is derived from rhodanine, and there is not any toxicity information about R-NA (CAS# 5718-83-2) on the material safety data sheet. The R-NA molecule has an additional acetic acid group which is assumed to be an active center of adsorption, and this group contributes to the solubility of the molecule in aqueous condition. Therefore, the molecule is expected to show good adsorption ability and corrosion inhibition efficiency.

The aim of this study is to investigate the inhibition efficiency of R-NA using electrochemical techniques for short and long immersion time and compare the results with rhodanine.[28]

2. EXPERIMENTAL SECTION

2.1. Preparation of Electrodes. The working electrode was cut from a copper rod, and the metal disc was coated with polyester except for its bottom surface with a surface area of 0.283 cm^2. The electrical conductivity was provided by copper wire. The surface of the working electrode was mechanically abraded using different grades of sand papers, which ended with the 1200 grade, prior to use. For each test, a freshly abraded electrode was used.

2.2. Test Solutions. The measurements were carried out in 0.5 M H_2SO_4 solution in the absence and the presence of various concentrations of R-NA (10.0 mM to 0.5 mM). A 0.5 M H_2SO_4 solution was prepared by dilution of 98% H_2SO_4 with distilled water. The chemical structure of R-NA is given in Figure 1. All the solutions were prepared by using analytical reagent grade H_2SO_4 and R-NA, in distilled water. All experiments were performed at 25 ± 1 °C in solutions open

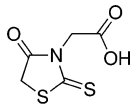

Figure 1. Chemical structure of Rhodanine-N-acetic acid.

Received: January 16, 2013
Revised: June 17, 2013
Accepted: June 24, 2013
Published: June 24, 2013

dx.doi.org/10.1021/ie400160x | *Ind. Eng. Chem. Res.* 2013, 52, 9709−9718

to the atmosphere under unstirred conditions. For each experiment, a freshly prepared solution was used.

2.3. Electrochemical Measurements. The electrochemical experiments were performed in a classical three-electrode cell assembly with copper as the working electrode, platinum foil of 1 cm × 1 cm as the counter electrode, and an Ag/AgCl (3 M KCl) as the reference electrode. All potential values were referred to as the Ag/AgCl reference electrode. A CHI 604 model computer controlled electrochemical analyzer (serial number: 6A721A) was used for the measurements. The working electrode was immersed in a test solution for 1 h to establish the steady state open circuit potential (E_{ocp}). After measuring the E_{ocp}, the electrochemical measurements were performed. The EIS experiments were conducted in the frequency range of 100 kHz to 0.003 Hz at open circuit potential. The amplitude was 0.005 V. The cathodic polarization curves were obtained in the potential ranges from E_{ocp} to −1.0 V (Ag/AgCl) with a scan rate of 0.001 V s^{-1}, and the anodic polarization curves were obtained in the potential ranges from E_{ocp} to 0.8 V (Ag/AgCl) with a scan rate of 0.001 V s^{-1}. LPR measurements were carried out by recording the electrode potential ±0.010 V around an open circuit potential with 0.001 V s^{-1} scan rate. The polarization resistance (R_p) was determined from the slope of current−potential curves obtained. Newly prepared electrodes as well as the test solutions were used for each experiment. All experiments were repeated at least three times.

The corrosion behavior of copper in 0.5 M H_2SO_4 solution in the presence and absence of 10.0 mM R-NA as a function of exposure time was also performed over 120 h. During the long-term tests, the working electrode was immersed in a beaker containing 200 mL of the test solution. After different immersion times, electrochemical measurements were performed under unstirring conditions.

2.4. Scanning Electron Microscopy Studies. In order to examine the changes in surface morphology of the electrodes covered with a thin film of R-NA, the electrodes were immersed in 200 mL of uninhibited and inhibited solutions. After 120 h waiting time, the electrodes were removed from the cells, washed with distilled water, and dried. The SEM images were taken using a Carl Zeiss Evo 440 SEM instrument at high vacuum and 10 kV EHT.

3. RESULTS AND DISCUSSION

3.1. Potentiodynamic Polarization Measurements. Potentiodynamic polarization curves of copper in the absence and the presence of various R-NA concentrations in 0.5 M H_2SO_4 solution after 1 h immersion time are shown in Figure 2. The related electrochemical parameters, open circuit potential (E_{ocp}), the potential hydrogen evolution starts (EH_2), diffusion limited current density of oxygen (i_{diff}), and the current densities at different over potentials are calculated and given in Table 1. The i_{diff} values were calculated by extrapolation of the linear region of cathodic curves corresponding to diffusion controlled reduction of dissolved oxygen. As it can be seen in Figure 2, it is not possible to evaluate the Tafel slopes as there are no visible linear regions that prevent linear extrapolation to corrosion potential (E_{corr}) of the polarization curves.

From the corresponding polarization curves presented in Figure 2, it is inferred that in the presence of R-NA as an inhibitor, the corrosion potential shifts toward the negative direction in comparison to the results obtained in the absence of the inhibitor, demonstrating the cathodic inhibition effect. It

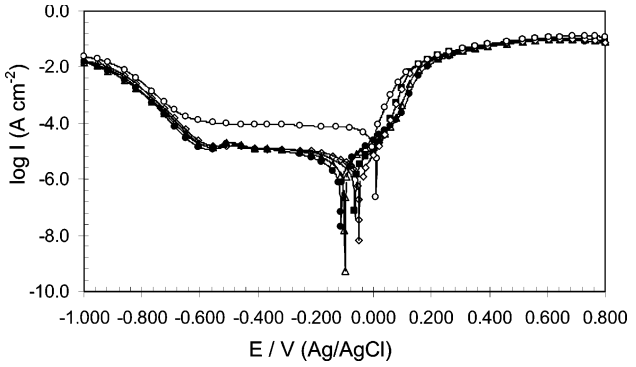

Figure 2. Polarization curves of copper electrode obtained in 0.5 M H_2SO_4 solution (○) and containing 0.5 (◊), 1.0 (■), 5.0 (Δ), and 10.0 mM (●) R-NA at 25 °C.

is also evidenced from the obtained curves that the R-NA predominantly controls the cathodic reaction.

As it is seen from Figure 2, it is observed an increase of anodic current starting from Eocp with increasing potential due to the dissolution of copper from the anodic polarization curve. The presence of R-NA in corrosive media with 10.0 mM to 0.5 mM concentration range has significantly changed the appearance of the curves. The current plateaus are observed for all inhibitor concentrations due to the adsorption of the R-NA molecules on the copper surface and a protective inhibitor layer formation. This current plateau disappears at more positive potentials with increasing current density due to the dissolution of Cu.[29] R-NA molecules adsorb on the metal surface and reduce the anodic current density at lower anodic potential regions (0.1 V (Ag/AgCl)). This anodic current density decreases with increasing R-NA concentration. Minimum anodic current density is observed at a concentration of 10.0 mM R-NA according to the obtained results.

In the evaluation of the cathodic branch of the current−potential curves for copper (Figure 2), the cathodic current density increases up to ∼−0.1 V (Ag/AgCl) due to the oxygen diffusion. The current plateaus are also observed between ∼−0.1 V and ∼−0.6 V (Ag/AgCl). This plateau appeared due to reduction of the dissolved oxygen or existence of the bearing diffusion to the cathode level. After the limit of the diffusion process at more negative potentials, the current density increases again with starting hydrogen evolution. The diffusion limited current density of oxygen plays a dominant role on copper corrosion process. In the presence of R-NA molecules in the corrosive media, the diffusion limited current density of oxygen decreases as it was shown in Table 1. It is almost the same for different concentrations of R-NA. The diffusion limited current density obtained from potentiodynamic polarization curves in the presence of R-NA molecules (10.0 mM) in the corrosive media (0.5 M H_2SO_4) was lower than in the presence of rhodanine molecules in the same environment. The diffusion limited current densities of oxygen in the presence of rhodanine and R-NA molecules are 222 μA cm^{-2}[28] 34.6 μA cm^{-2}, respectively. This decrease in the limiting current may be due to organic additives adsorption on the electrode surface. The concentration of R-NA molecules at the electrode solution interface may decrease in the diffusion of copper ions (Cu^{2+}). Besides, the anchorage of the solution to the electrode surface by organic molecules hinders the flow of the solution past the electrode surface with a consequent decrease in the limiting current as well as by the possible formation of copper

dx.doi.org/10.1021/ie400160x | Ind. Eng. Chem. Res. 2013, 52, 9709−9718

Table 1. Electrochemical Parameters for Copper Electrode Determined from Polarization Measurements in 0.5 M H_2SO_4 Solution without and with Various Concentrations of R-NA after 1 h Exposure

inhibitor	C/mM	E_{ocp}/V (Ag/AgCl)	EH_2/V (Ag/AgCl)	i_{diff}/μA cm^{-2}	$i_{-0.7\ V}$/μA cm^{-2}	$i_{0.1\ V}$/μA cm^{-2}	$i_{0.7\ V}$/mA cm^{-2}
R-NA	blank	0.004	−0.663	793.0	1269	16070	454
	0.5	−0.046	−0.619	36.0	737	7670	350
	1.0	−0.058	−0.610	41.8	592	7842	372
	5.0	−0.093	−0.605	39.2	468	1972	355
	10.0	−0.111	−0.588	34.6	370	1001	306

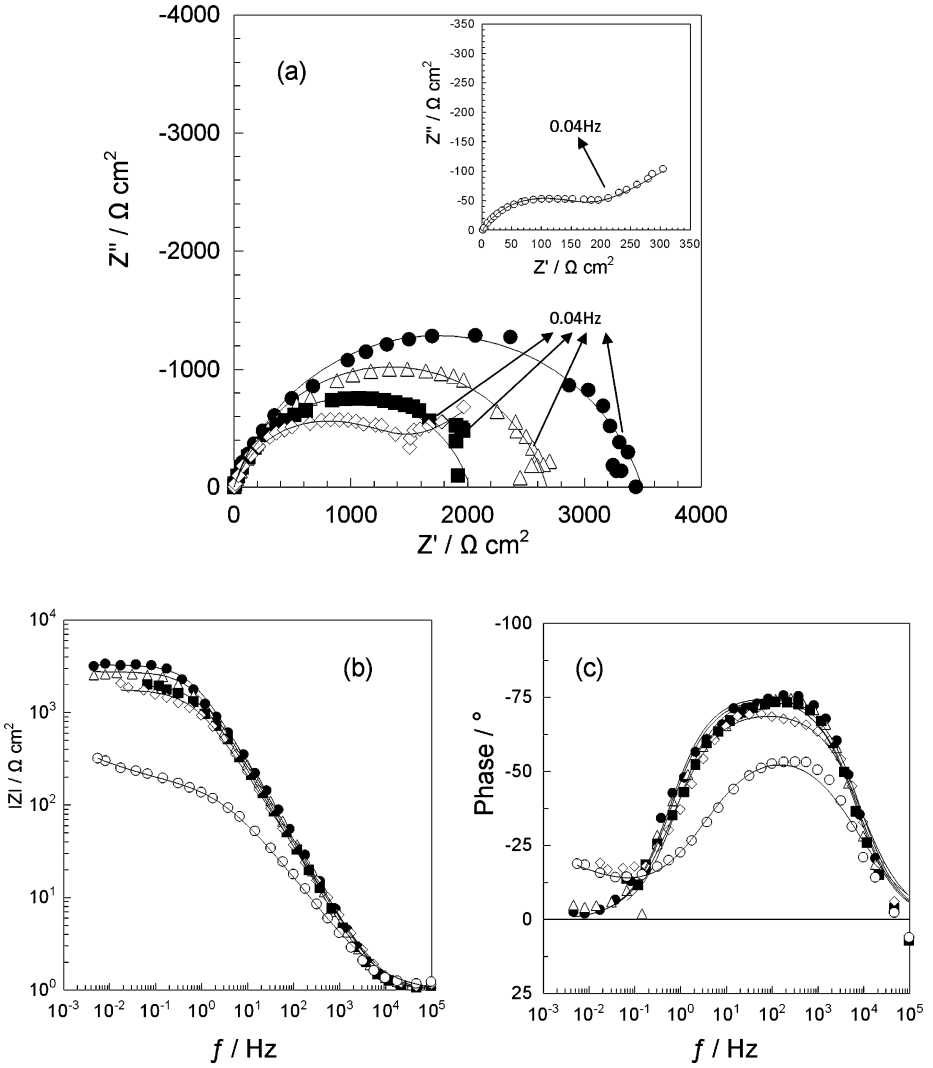

Figure 3. Nyquist (a), Bode (b), and phase angle (c) plots of copper electrode obtained in 0.5 M H_2SO_4 solution (○) (inset) and containing 0.5 (◊), 1.0 (■), 5.0 (Δ), and 10.0 mM (●) R-NA (solid lines show fitted results).

complexes in the limited space of the diffusion layer where adsorbed R-NA concentration is high and Cu^{2+} concentration is low. It can be concluded that the ability of R-NA and rhodanine as a corrosion inhibitors is enhanced as the dissolved O_2 content is increased.[30] This permits in distinguishing the contribution of O_2 reduction from that of hydrogen evolution. The observed limiting current density for O_2 reduction was dependent on mass transport. The obtained diffusion current densities, as seen in Table 1, showed that the O_2 reduction process is mainly under diffusion control. This suggests that the cathodic reaction is the four-electron reduction of dissolved O_2 according to the following reaction:

$$O_2 + 2H_2O + 4e^- \leftrightarrow 4OH^- \quad (1)$$

In aerated acidic solutions, the presence of dissolved O_2 enhances the cathodic reaction due to O_2 reduction (eq 1). This causes copper to corrode rapidly to form a compact and porous film of cuprous oxide, and then, this cuprous-based species will act to catalyze the O_2 reduction reaction.[31] Therefore, the R-NA molecule could be used due to reduced oxygen diffusion current densities in the aerated solution. The addition of the inhibitor to the corrosive media also shifts the potential hydrogen evolution starts toward less negative potential, and this behavior is more pronounced with increasing inhibitor concentration. The potential hydrogen evolution

dx.doi.org/10.1021/ie400160x | Ind. Eng. Chem. Res. 2013, 52, 9709−9718

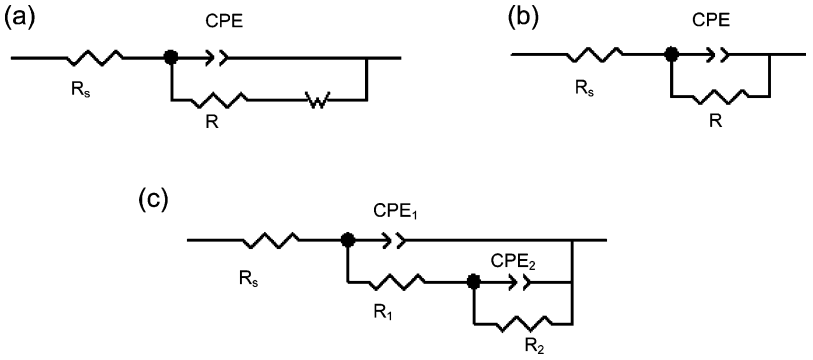

Figure 4. Electrical equivalent circuit diagram used for modeling copper/solution interface in 0.5 M H_2SO_4 solution in the absence and presence of 0.5 mM R-NA (a), in the presence of 10.0, 5.0, and 1.0 mM R-NA and after 4 h immersion time (b), and in the absence and presence of 10.0 mM R-NA after 120 h immersion time (c).

Table 2. Electrochemical Parameters for Copper Electrode Corresponding to the EIS and LPR Data in 0.5 M H_2SO_4 Solution in the Absence and Presence of Various Concentrations Containing R-NA at 25 °C

		EIS				LPR	
	C/mM	R_p (Ω cm^2)	CPE_{dl} (μF cm^{-2})	n	η%	R_p (Ω cm^2)	η%
R-NA	blank	166	852.9	0.66		195	
	0.5	1358	142.0	0.82	87.8	2057	90.5
	1.0	2019	25.0	0.82	91.8	2178	91.0
	5.0	2678	15.2	0.83	93.8	2322	91.6
	10.0	3502	12.8	0.81	95.3	3291	94.0

starts and limited oxygen diffusion current results show that R-NA inhibits a cathodic reaction with a stable protective film over the copper surface. The cathodic current density increases significantly with increasing the R-NA concentration at the higher cathodic potential region (−0.7 V (Ag/AgCl)). These results indicate that the R-NA has a stronger influence on the oxygen reduction than on the Cu oxidation reaction,[32] and it may adsorb on the copper surface with a protective inhibitor film layer formation.

3.2. Electrochemical Impedance Spectroscopy (EIS) Measurements. Figure 3 presents the Nyquist and Bode plots of copper in 0.5 M H_2SO_4, in the absence and presence of R-NA at various concentrations. The Nyquist plot obtained in a blank solution is given as the inset in Figure 3a. As it is seen from the inset in Figure 3a, the Nyquist plots obtained in the absence of R-NA and the lowest concentration of R-NA exhibited a Warburg impedance containing a capacitive loop in the high frequency region and following a straight line in low frequencies.[7,33] The high frequency capacitive loop is related to the charge transfer resistance (R_{ct}) and diffuse layer resistance (R_d).[29] The low frequency straight line indicates that the corrosion process involves the transport of reactants from the bulk solution to the copper/solution interface or transport of soluble corrosion products from the interface of the bulk solution in the early stage of corrosion. In the copper corrosion in aerated H_2SO_4 solutions at E_{corr}, the anodic reaction is copper dissolution, and cathodic reaction is oxygen reduction being the hydrogen discharge current density negligible as compared to oxygen reduction current density.[34] Then, the Warburg impedance can be attributed to oxygen transport from the bulk solution to the copper surface.[35] The Warburg impedance only displays in the bulk solution and the presence of R-NA at a concentration of 0.5 mM. In the other concentrations, the Warburg impedance disappears, and the Nyquist plots only display a depressed capacitive loop. Moreover, the size of the capacitive significantly increases with the further increase of the R-NA concentration until 10.0 mM. The Nyquist plots changes, including both the increase of capacitive loop and the disappearance of the Warburg impedance, indicate that inhibitor molecules more and more adsorb on the copper surface by increasing the concentration of R-NA. This situation restricts the oxygen diffusion to the solution-metal interface and so increases the reaction-kinetic resistance and reduces the corrosion rate. Moreover, this stage shows that a barrier gradually forms on the surface. The barrier is probably related to formation of the film of the $[Cu(R-NA)_n^+]$ complex.

The Bode and phase angle plots for the copper in 0.5 M H_2SO_4 solution containing various inhibitor concentrations after 1 h of immersion are given in Figure 3b and c, respectively. As seen from Figure 3b and c, Bode and phase angle plots refer to the existence of an equivalent circuit that contains a two time constant phase element (0.5 mM R-NA) and a one time constant (in the other concentrations of R-NA) in the metal/solution interface.

The EIS data were fitted to the equivalent circuit models used for modeling copper/solution interface in 0.5 M H_2SO_4 solution in the absence and presence of 0.5 mM R-NA after 1 h immersion time (Figure 4a), in the presence of 10.0, 5.0, and 1.0 mM R-NA after 1 h immersion time (Figure 4b), in the presence of 10.0 mM R-NA after 4 h immersion time (Figure 4b), and in the presence of 10.0 mM R-NA after a longer immersion time (120 h) (Figure 4c). In equivalent circuit models in Figure 4, R_s represents solution resistance between the working and reference electrodes, CPE is a power-law-dependent capacity term known as the constant phase element that may be brought by surface roughness,[36] CPE is used in place of double layer capacitance, C_{dl}, to represent the nonideal capacitive behavior of the double layer. CPE_1 corresponds to film capacitance, and CPE_2 corresponds to double layer

dx.doi.org/10.1021/ie400160x | Ind. Eng. Chem. Res. 2013, 52, 9709−9718

capacitance. R_{ct} represents charge transfer resistance and corresponds to the resistance between the metal and outer Helmholtz plane.[37,38] In the present study, the difference in real impedance at low and high frequencies is considered as the polarization resistance (R_p). R_1 is film resistance (R_f), R_2 represents the pore resistance (R_{por}, corresponds to uncovered regions and pores), W is Warburg impedance.[39−41] The fitting parameters of impedance data obtained by using the equivalent circuit models in Figure 4 are listed in Tables 2 and 3. $R = R_{ct} +$ R_d for Figure 4a, $R = R_{ct} + R_d + R_a + R_f$ for Figure 4b, and $R_1 = R_{por}$ ($R_{por} = R_{ct} + R_d + R_a$) $R_2 = R_f$ for Figure 4c. The R_p values obtained from the LPR technique were added to Table 2 with corresponding inhibition efficiencies (η). η is calculated using R_p values as follows

Table 3. Electrochemical Impedance Parameters and the Corresponding Inhibition Efficiencies for Copper Electrode in 0.5 M H_2SO_4 Solution in the Absence and Presence of 10.0 mM R-NA after Different Immersion Time at 25 °C

	R-NA		blank	
EIS	4 h	120 h	4 h	120 h
R_1/Ω cm^2	2720	76.6	26.8	125.7
CPE_1/μF cm^{-2}	198.2	201.7	343.7	733.4
n_1	0.86	0.85	0.75	0.74
R_2 /Ω cm^2	-	839.5	-	759.7
CPE_2/μF cm^{-2}	-	36.3	-	11363.0
n_2		0.98		0.57

$$\eta\% = \left(\frac{R'_p - R_p}{R'_p}\right) \times 100 \quad (2)$$

where R'_p and R_p are polarization resistance with and without an inhibitor, respectively.

The R_p and η values obtained from the LPR measurements are comparable and run parallel with those obtained from the EIS measurements. It is apparent that corrosion resistance and inhibition efficiency of the copper increase significantly in the presence of R-NA suggesting the enhancement of adsorption of inhibitor molecules on the copper and blocking the metal surface efficiently. The same properties were observed in the presence of rhodanine.[28] It is seen that the profile of Nyquist and Bode plots in the presence of 10.0 mM rhodanine is similar with the plots observed when 10.0 mM R-NA is added to 0.5 M H_2SO_4 solution. However, the lower polarization resistance appears in the presence of R-NA. This behavior may attribute to the adsorption of more rhodanine molecules on copper surface. The thickness of the film formed increased when rhodanine is added to corrosive media in comparison to that observed in the presence of R-NA. Both rhodanine and R-NA cause a remarkable decrease in the corrosion rate. Generally, the phenomenon of adsorption is influenced by the nature of metal and molecular structure of the inhibitor. In comparison to the R-NA and rhodanine inhibition efficiencies determined from EIS are close to each other, which are 95.3% and 98.8%[28] in the presence of 10.0 mM inhibitor concentration, respectively. This efficiency difference can be explained with the presence of the (−COOH) group in conjugation with an aromatic ring on the R-NA molecule. The presence of the (−COOH) group in an aromatic ring may be influenced by

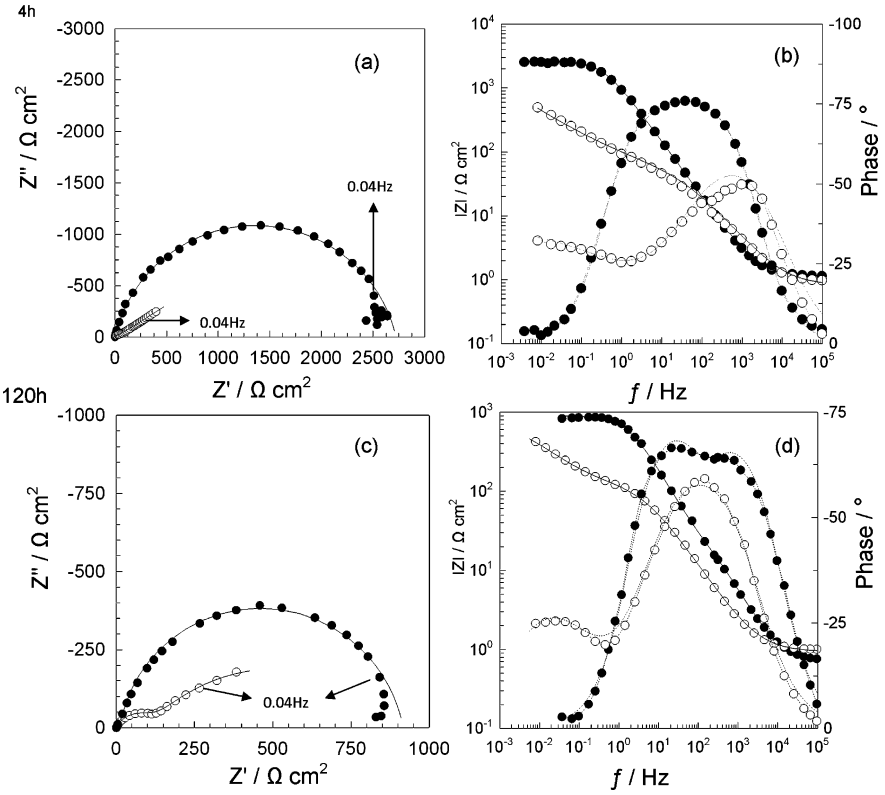

Figure 5. Nyquist (a,c) and Bode (b,d) plots of copper electrodes in 0.5 M H_2SO_4 solution in the absence (○) and presence of 10.0 mM R-NA (●) after 4 and 120 h exposure time (solid lines show fitted results).

dx.doi.org/10.1021/ie400160x | Ind. Eng. Chem. Res. 2013, 52, 9709−9718

electron density on the R-NA molecules. The R-NA molecule has an additional acetic acid group according to the rhodanine molecule. This group contributes the adsorption center and the solubility to the molecule in aqueous media. R-NA is more soluble in aqueous media than the rhodanine molecule.

The kinetic of the corrosion inhibitor is another important role in assessing the stability of inhibitive behavior of inhibitors, so it is necessary to evaluate the inhibition efficiency of the inhibitor for a long immersion time. In the present study, the effect of immersion time (4−120 h) on corrosion inhibition of copper in 0.5 M H_2SO_4 in the absence and presence of R-NA at the optimum concentration (10.0 mM) for 4−120 h immersion time at the temperature 25 °C was also studied by using EIS. Nyquist and Bode diagrams of copper in uninhibited and inhibited solutions, after different exposure times, are shown in Figure 5. As it can be seen from Figure 5, the Nyquist plot for the blank solution appears as a capacitive loop in the high frequency region and a straight line in the low frequency region after 4 and 120 h exposure times. In the presence of R-NA at 4 h, one capacitive loop is observed in the Nyquist plot, and one time constant appears in the Bode plot (Figure 5a,c). However, in the presence of R-NA at 120 h, two capacitive loops are observed in the Nyquist plot and two time constants appear in the Bode plot (Figure 5b,d). After 120 h, the polarization resistance obtained from the Nyquist diagram containing two capacitive loops for the uninhibited solution increases as a result of the formation of the copper oxide layer. In the presence of R-NA, the diameter of the semicircle is recorded in the presence of the inhibitor decrease significantly as compared to 4 h exposure times, because of the moving away from the metal surface of inhibitor molecules upon exposure. The values of polarization resistance, *n*, and *CPE* values corresponding to the EIS data as being associated with over 120 h immersion time are given in Table 3. It is clear from Table 3 that the R_p values decrease in the inhibited solution compared to uninhibited ones until 120 h of exposure time as a result of an increase in the dissolution of the metal surface and the reduction of inhibitor molecules sticking to the metal surface. After 120 h, the R_p values of copper in the absence of R-NA attain higher values in comparison to that obtained from 4 h of immersion. This indicates that the copper is more passive after 120 h immersion due to the accumulated corrosion products on its surface.

3.3. Potentiodynamic Polarization Measurements after 120 h Exposure Time. Figure 6 shows the potentiodynamic polarization curves of copper in the absence and presence of 10.0 mM R-NA in acidic solutions after 120 h exposure time. In the evaluation of the cathodic branch of the current−potential curves for copper, the cathodic current plateau is not observed at this branch. This region shifts anodic branch due to the formation of a passive layer on the surface. At the same time, the diffusion limited current density of oxygen region narrow for inhibited solution. As it is seen from Figure 6, both anodic and cathodic current densities reduce considerably, and open circuit potential shift to nobler potentials at inhibited solution in comparison with a bare sample. The decreasing current densities in the case of R-NA can be explained by the physical barrier property of the inhibitor. Polarization curves for uninhibited and inhibited samples clearly show that R-NA provides a great protection for copper in 0.5 M H_2SO_4 solution.

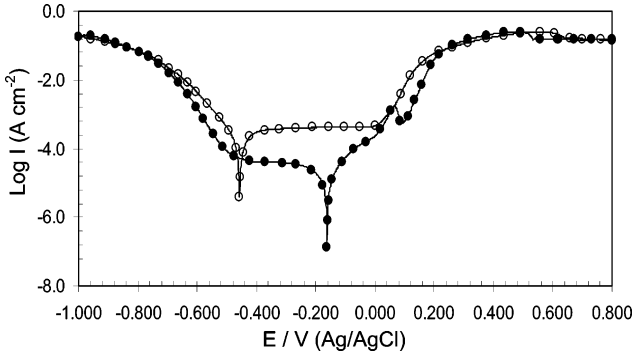

Figure 6. Polarization curves of copper electrodes in 0.5 M H_2SO_4 solution in the absence (○) and presence of 10.0 mM R-NA (●) after 120 h exposure time.

3.4. Change of Open Circuit Potential with Immersion Time. The variation of E_{ocp} of copper as a function of exposure time ($E_{ocp\text{-}t}$) was measured versus Ag/AgCl reference electrode in the 0.5 M H_2SO_4 solution in the absence and presence of 10.0 mM R-NA. The obtained data are presented graphically in Figure 7. As it can be seen from Figure 7, the E_{ocp} of copper observed in blank solution shifts toward more negative potentials. This behavior may be a result of adsorption of SO_4^{2-} ions on copper surface and formation of soluble $CuSO_4$ species. The similar behavior was reported for copper in chloride containing solutions. The shift in E_{ocp} toward more negative potentials after the addition of R-NA may be suggested as the influence of the inhibitor on the cathodic process. The shift in E_{ocp} of copper toward more negative potential attributed to the adsorption of R-NA molecules on the active corrosion sites.[28,42] Up to 48 h, the shift in E_{ocp} toward more positive potentials after the addition of R-NA may be explained based on dissolution of copper and oxide layer film formed at the metal surface as a result of desorption from the metal surface of R-NA molecules. The values of E_{ocp} are −0.12 V and −0.11 V (Ag/AgCl) in the presence of rhodanine[28] and R-NA, respectively, after 1 h immersion time. The similar E_{ocp} values were obtained, indicating that the reaction mechanism for the corrosion of copper is almost identical.

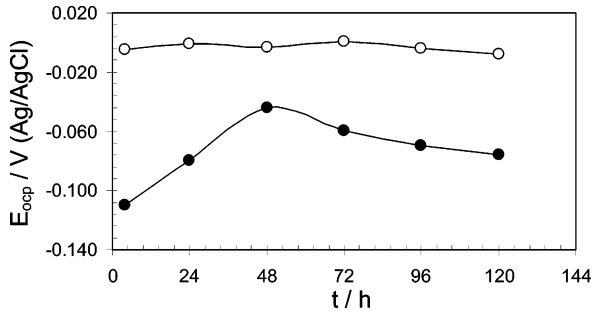

Figure 7. The change of open circuit potential as a function of exposure time in 0.5 M H_2SO_4 (○) and containing 10.0 mM R-NA (●) solutions.

3.5. Adsorption Isotherm and Thermodynamic Consideration. To understand the mechanism of corrosion inhibition, the adsorption behavior of the organic molecule on the metal surface must be known. When a simple adsorption behavior is assumed for R-NA, a direct relationship between inhibition efficiency and surface coverage of the inhibitor, θ, takes place, and the electrochemical impedance spectroscopy data are used to evaluate the surface coverage values, which are given by eq 3

dx.doi.org/10.1021/ie400160x | Ind. Eng. Chem. Res. 2013, 52, 9709−9718

$$\theta = \left(\frac{R'_p - R_p}{R'_p} \right) \quad (3)$$

where R_p and R'_p are the polarization resistance values without and with the inhibitor, respectively. The surface coverage values (θ) were tested graphically to allow fitting of a suitable adsorption isotherm including Langmuir, Frumkin, Temkin, etc. The plots of C_{inh}/θ against C_{inh} for R-NA give a straight line with an almost unit slope (Figure 8), indicating that the R-NA

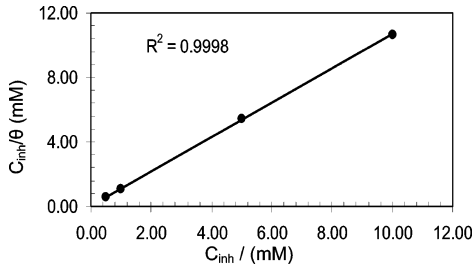

Figure 8. Langmiur adsorption plot of copper in 0.5 M H_2SO_4 solution containing different concentrations of R-NA at 25 °C.

compounds obey the Langmuir adsorption isotherm on the copper in 0.5 M H_2SO_4

$$\frac{C_{inh}}{\theta} = \frac{1}{K_{ads}} + C_{inh} \quad (4)$$

where K_{ads} is the equilibrium constant of the adsorption process. The slope of the straight line (K_{ads}) is found to be 1.88 × 10^4 M^{-1} suggesting that the adsorbed inhibitor molecules form the monolayer on the copper surface and there is no interaction among the adsorbed inhibitor molecules.[43] On the other hand, the relatively high value of adsorption equilibrium constant reflects the high adsorption ability of R-NA on the copper surface.[44,45] The strong correlations (R^2 = 0.9998) confirm the validity of this approach. The standard free energy of adsorption (ΔG°_{ads}) can be calculated from the equation

$$\Delta G^\circ_{ads} = -RT(\ln 55.5K_{ads}) \quad (5)$$

where R is the gas constant (8.314 J mol^{-1} K^{-1}), T is the absolute temperature (K), and the value 55.5 is the concentration of water in solution expressed in mol L^{-1}. The calculated values of the adsorption parameters the standard free energy of adsorption (ΔG°_{ads}) is −34.33 kJ mol^{-1}. It is well-known that values of ΔG°_{ads} in the order of −20 kJ mol^{-1} or lower indicate a physisorption; those about −40 kJ mol^{-1} or higher involve charge sharing or a transfer from the inhibitor molecules to the metal surface to form a coordinate type of bond.[46,47] The ΔG°_{ads} value of rhodanine[28] (about −38.81 kJ mol^{-1}) was found to be more negative than that for R-NA. The adsorption equilibrium constant is also higher for rhodanine[28] (1.15 × 10^5 M^{-1}) in comparison to R-NA (1.88 × 10^4 M^{-1}) which indicates the easier adsorption of rhodanine[28] on copper. The adsorption mechanism of the rhodanine and R-NA on the copper surface in 0.5 M H_2SO_4 solution can be described both as physisorption and chemisorption; however, the steric effect of R-NA may also play a role here and explain its less negative ΔG°_{ads} value. These result in the rhodanine easier film formation on a copper surface. This justifies the higher corrosion inhibition efficiencies of rhodanine in comparison to R-NA.

3.6. Inhibition Mechanism. The transition of the metal/solution interface from a state of active dissolution to the passive state is attributed to the adsorption of the inhibitor molecules and the metal surface, forming a protective film. The rate of adsorption is usually rapid, and, hence, the reactive metal surface is shielded from the aggressive environment.[48] Adsorption of an inhibitor can be described by two main types of interactions: physical adsorption and chemisorption. In general, physical adsorption requires the presence of both the electrically charged surface of the metal and charged species in solution. The surface charge of the metal is due to the electric field existing at the metal/solution interface. A chemisorption process, on the other hand, involves charge sharing or charge transfer from the inhibitor molecules to the metal surface to form a coordinate type of a bond. This is possible in the case of a positive as well as a negative charge of the surface. The presence of a transition metal, having vacant, low-energy electron orbital (Cu^+ and Cu^{2+} in our case) and of an inhibitor with molecules having relatively loosely bound electrons or heteroatoms with a lone pair of electrons is necessary.[49]

Ashassi-Sorkhabi indicates that organic molecules may adsorbed on the metal surface in four types:[50] (i) electrostatic attraction between the charged molecules and the charged metal, (ii) interaction of unshared electron pairs in the molecule with the metal, (iii) interaction of π-electrons with the metal, and (iv) a combination of the types i-iii. Accordingly, all of them have an inhibiting effect.

According to Mattson and Bockris, the anodic dissolution of copper in sulfuric acid solution follows the mechanism given below[51]

$$Cu \leftrightarrow Cu^+_{ads} + e^- \quad \text{(fast step)} \quad (6)$$

$$Cu^+_{ads} \leftrightarrow Cu^{2+} + e^- \quad \text{(slow)} \quad (7)$$

where Cu^+_{ads} is an adsorbed species at the copper surface. The reaction step 7 is generally the rate determining step and controlled by diffusion of soluble Cu^{2+} species from the electrode surface to the bulk solution. The slope variation in the inhibited solution indicates a change in the copper dissolution. Unlike the two-electron electrodissolution mechanism, copper in the presence of R-NA could be electrooxidized primarily to Cu^+_{ads} and is able to form slightly soluble $[Cu\text{-}R\text{-}NA_n]^+_{ads}$ complexes as the main electrooxidation products in the presence of a bare surface.[52,53] The possible reaction is as follows

$$Cu^+ + nR\text{-}NA \leftrightarrow [Cu\text{-}R\text{-}NA_n]^+_{ads} \quad (8)$$

where n is the number of adsorbed R-NA molecules on the copper surface. This molecule gets chemisorbed on the surface of copper and forms a chelate with Cu^+ ions already existing on the copper surface due to initial corrosion of copper. The values of ΔG°_{ads} indicate that the adsorption of the studied organic inhibitor on the copper surface from 0.5 M H_2SO_4 solution is more chemical than physical.

In the first statement of Ashassi-Sorkhabi, inhibitor molecules can also be adsorbed on the copper surface via electrostatic interaction between the charged metal surface and charged inhibitor molecules. The standard free energy of adsorption value is modestly lower at −40 kJ mol^{-1} and should indicate the contribution of physical adsorption. The inhibition effect of R-NA in sulfuric acid solution can be explained as follows: R-NA might be protonated in the acid solution as follows:

dx.doi.org/10.1021/ie400160x | Ind. Eng. Chem. Res. 2013, 52, 9709−9718

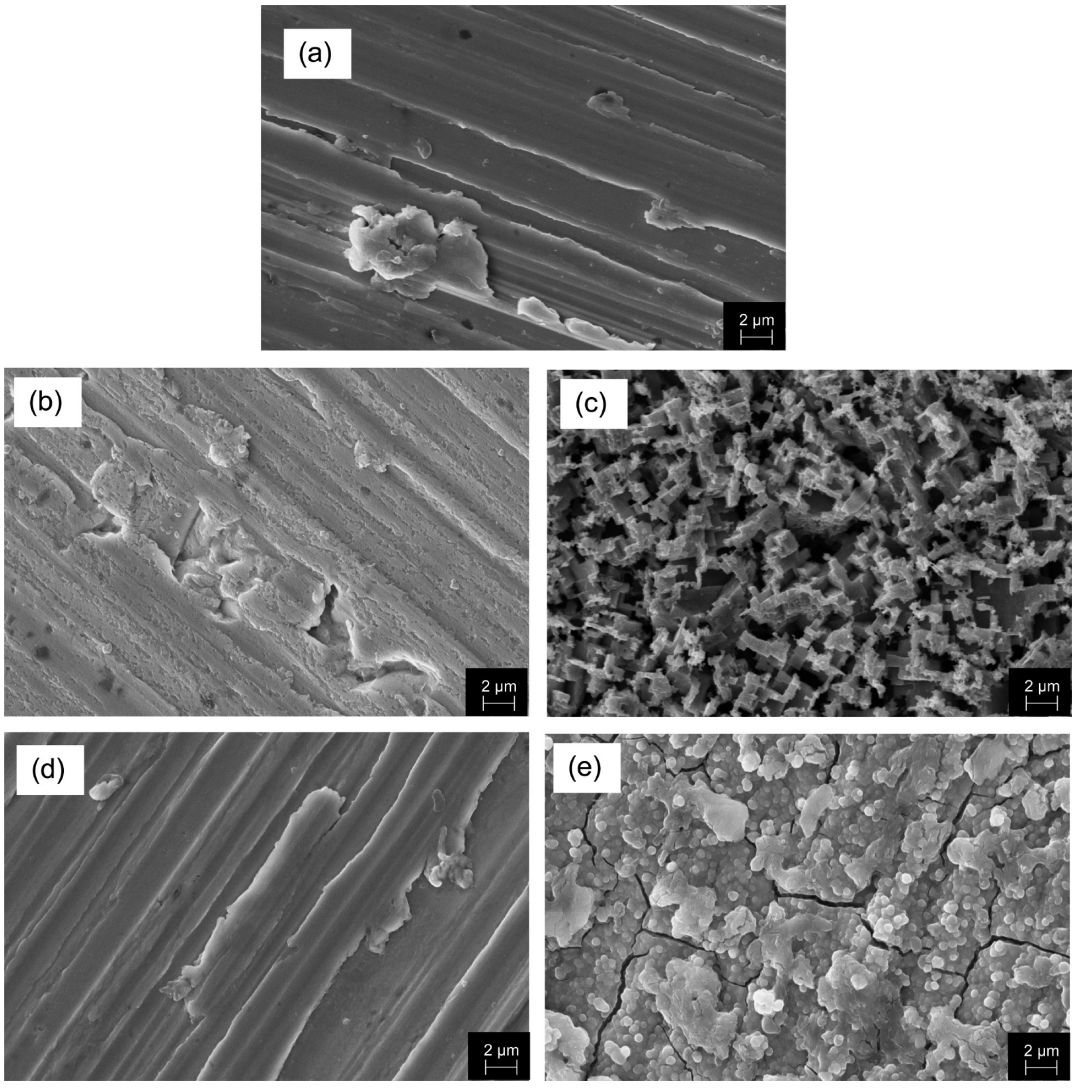

Figure 9. SEM images of copper samples: after freshly polished (a), after immersion for 1 h (b)[28] and 120 h (c) in 0.5 M H_2SO_4 solution without inhibitor, and after immersion for 1 h (d) and 120 h (e) in 0.5 M H_2SO_4 solution in the presence of 10.0 mM R-NA.

$$\text{R-NA} + H^+ \leftrightarrow \text{R-NAH}^+ \quad (9)$$

The protonated R-NA can be adsorbed on the metal surface by means of electrostatic interaction between SO_4^{2-} (which act as a bridge between the metal surface and the solution) and protonated R-NA. The adsorption of protonated R-NA molecules reduces the rate of hydrogen, oxygen evolution reactions, and anodic dissolution of copper. The inhibition mechanism of rhodanine[28] is similar to R-NA, because the products $[\text{Cu-Rdn}_n]^+_{ads}$ and $RdnH^+$ occurred in the same way. As described above, in the inhibition mechanism of rhodanine,[28] SO_4^{2-} ions was first adsorbed onto the positively charged metal surface. Then, the inhibitor molecules were adsorbed through electrostatic interactions between the negatively charged metal surface and positively charged inhibitor molecules

3.7. Scanning Electron Microscopy Studies. Scanning electron microscopy studies of the samples in the absence and presence of the inhibitor after 1 and 120 h immersions were performed to examine the nature of the film on the surface. Figure 9 shows the SEM images of the copper exposed to 0.5 M H_2SO_4 solution in the absence and presence of R-NA. For comparison, the SEM image of the freshly polished copper was also given. The polishing stretches were visible on the surface of a freshly polished copper surface as it was shown in Figure 9a. It could be observed from Figure 9b that the copper surface after 1 h immersion was damaged with the attacking by H_2SO_4 in the absence of the inhibitor. Some pits are seen on the surface. After 120 h immersion, the copper surface was strongly damaged with the increasing number and the depth of the pits (Figure 9c). The corrosion products completely covered the surface, and the surface layer is extensively rough. A large number of pits with large size and high depth distributed over the surface are seen from Figure 9c. The influence of the inhibitor addition on the copper in 0.5 M H_2SO_4 solution is shown in Figure 9d,e. The surface is free from pits, and it is smooth (Figure 9d); even the original polishing scratches are seen. This clearly reveals that the rate of corrosion is suppressed in the presence of R-NA. After 120 h immersion in inhibited solution (Figure 9e), some cracks and corrosion products appeared on the surface. There is still a protective layer and much less damage on the surface. Therefore, it can be concluded that the smooth and much less corroded morphology of specimens may be attributed to the adsorption of R-NA on the metal surface and formation of a protective

dx.doi.org/10.1021/ie400160x | Ind. Eng. Chem. Res. 2013, 52, 9709−9718

inhibitor layer. In order to characterize the surface images in the presence of both rhodanine derivates, SEM images were compared after 1 h immersion in 0.5 M H_2SO_4 solution with both rhodanine derivates. In the presence of R-NA, the surface looks relatively uneven compared to that immersed in rhodanine containing solutions (Figure 9d).[28] Polishing lines can be clearly seen in the micrograph after addition of both rhodanine derivates.[28] Both inhibitor molecules adsorb on the copper surface and a smoother surface forms when compared to the surface treated with the uninhibited acid solution.

4. CONCLUSIONS

Rhodanine-N-acetic acid was electrochemically investigated as a corrosion inhibitor for copper in 0.5 M H_2SO_4 solution. The data were also compared to the results of previously studied rhodanine cases.[28]

The main conclusions that are drawn from this study are as follows:

1. Experimental investigations of the studied R-NA and rhodanine[28] show that both rhodanine derivates reduce the corrosion rate of copper remarkably as their concentration increase. Their inhibition efficiencies are both concentration and immersion time dependent. The highest inhibitor efficiency is obtained at 10.0 mM rhodanine and R-NA concentration.

2. Polarization studies show that this class of compounds acts as mixed-type inhibitors, but R-NA has a more predominant cathodic effect than rhodanine has.[28]

3. The adsorption of both inhibitor molecules from acid solution obeys Langmuir adsorption isotherm. The adsorption equilibrium constant is higher for rhodanine[28] in comparison to R-NA, which indicates the easier adsorption of rhodanine[28] on copper.

4. The calculated standard free energies of adsorptions have been found be close to −40 kJ mol^{-1}, which can be explained as chemical rather than physical adsorption. The ΔG°_{ads} value of rhodanine[28] was found to be more negative than that for R-NA.

5. The high resolution SEM images showed the corrosion of the copper is mainly through pitting and the addition of both rhodanine derivates to the aggressive solutions results through the formation of a protective film on copper surface. In case of the solution containing rhodanine,[28] the protection film on the copper surface was the more compact and protected the surface of copper better against the attack of the aggressive environment.

AUTHOR INFORMATION

Corresponding Author

*Phone:+90-322-338-6081. Fax: +90-322-338-6070. E-mail: alidoner27@gmail.com.

Notes

The authors declare no competing financial interest.

ACKNOWLEDGMENTS

The authors are greatly thankful to the Çukurova University Research Fund for financial support (Project Number: FEF2011BAP12).

REFERENCES

(1) Nunez, L.; Reguera, E.; Corvo, F.; Gonzalez, E.; Vazquez, C. Corrosion of copper in seawater and its aerosols in a tropical island. *Corros. Sci.* **2005**, *47*, 461.

(2) Otsuka, R.; Uda, M. Cathodic corrosion of Cu in H_2SO_4. *Corros. Sci.* **1969**, *9*, 703.

(3) Stupnisek-Lisac, E.; Gazivoda, A.; Madzarac, M. Evaluation of non-toxic corrosion inhibitors for copper in sulphuric acid. *Electrochem. Acta* **2002**, *47*, 4189.

(4) Khaled, K. F.; Hackerman, N. Ortho-substituted anilines to inhibit copper corrosion in aerated 0.5 M hydrochloric acid. *Electrochem. Acta* **2004**, *49*, 485.

(5) Christy, A. G.; Lowe, A.; Otieno-Alego, V.; Stoll, M.; Webster, R. D. Voltammetric and Raman microspectroscopic studies on artificial copper pits grown in simulated potable water. *J. Appl. Electrochem.* **2004**, *34*, 225.

(6) Otmacic, H.; Telegdi, J.; Papp, K.; Stupnisek-Lisac, E. Protective properties of an inhibitor layer formed on copper in neutral chloride solution. *J. Appl. Electrochem.* **2004**, *34*, 545.

(7) Ma, H.; Chen, S.; Niu, L.; Zhao, S.; Li, S.; Li, D. Inhibition of copper corrosion by several Schiff bases in aerated halide solutions. *J. Appl. Electrochem.* **2002**, *32*, 65.

(8) Zucchi, F.; Trabanelli, G.; Fonsati, M. Tetrazole derivatives as corrosion inhibitors for copper in chloride solutions. *Corros. Sci.* **1996**, *38*, 2019.

(9) Wang, C.; Chen, S.; Zhao, S. Inhibition effect of AC-treated, mixed self-assembled film of phenylthiourea and 1-dodecanethiol on copper corrosion. *J. Electrochem. Soc.* **2004**, *151*, B11−B15.

(10) Kendig, M.; Jeanjaquet, S. Cr(VI) and Ce(III) inhibition of oxygen reduction on copper. *J. Electrochem. Soc.* **2002**, *149*, B47−B51.

(11) Ma, H. Y.; Yang, C.; Yin, B. S.; Li, G. Y.; Chen, S. H.; Luo, J. L. Electrochemical characterization of copper surface modified by n-alkanethiols in chloride-containing solutions. *J. Appl. Surf. Sci.* **2003**, *218*, 144.

(12) Otmacic, H.; Stupnisek-Lisac, E. Copper corrosion inhibitors in near neutral media. *Electrochim. Acta* **2003**, *48*, 985.

(13) Elmorsi, M. A.; Hassanein, A. M. Corrosion inhibition of copper by heterocyclic compounds. *Corros. Sci.* **1999**, *41*, 2337.

(14) Scendo, M.; Poddebniak, D.; Malyszko, J. Indole and 5-chloroindole as inhibitors of anodic dissolution and cathodic deposition of copper in acidic chloride solutions. *J. Appl. Electrochem.* **2003**, *33*, 287.

(15) Dafali, A.; Hammouti, B.; Touzani, R.; Kertit, S.; Ramdani, A.; El Kacemi, K. Corrosion Inhibition of copper in 3% NaCl solution by new bipyrazolic derivatives. *Anti-Corros. Methods Mater.* **2002**, *49*, 96.

(16) Zhang, Q.; Hua, Y. Corrosion inhibition of aluminum in hydrochloric acid solution by alkylimidazolium ionic liquids. *Mater. Chem. Phys.* **2010**, *119*, 57.

(17) Abd El-Maksoud, S. A. Some phthalazin derivatives as non toxic corrosion inhibitors for copper in sulphuric acid. *Electrochim. Acta* **2004**, *49*, 4205.

(18) Solmaz, R.; Kardaş, G.; Yazıcı, B.; Erbil, M. Inhibition effect of rhodanine for corrosion of mild steel in hydrochloric acid solution. *Prot. Met.* **2005**, *41*, 581.

(19) Solmaz, R.; Kardaş, G.; Yazıcı, B.; Erbil, M. Rhodanine inhibition effect on the corrosion of a mild steel in acid along the exposure time. *Prot. Met.* **2007**, *43*, 476.

(20) Yüce, A. O.; Solmaz, R.; Kardaş, G. Investigation of inhibition effect of rhodanine-N acetic acid on mild steel corrosion in HCl solution. *Mater. Chem. Phys.* **2012**, *131*, 615.

(21) Döner, A.; Kardaş, G. N-Aminorhodanine as an effective corrosion inhibitor for mild steel in 0.5 M H_2SO_4. *Corros. Sci.* **2011**, *53*, 4223.

(22) Abdallah, M. Rhodanine azosulpha drugs as corrosion inhibitors for corrosion of 304 stainless steel in hydrochloric acid solution. *Corros. Sci.* **2002**, *44*, 717.

(23) Altunbaş, E.; Solmaz, R.; Kardaş, G. Corrosion behaviour of polyrhodanine coated copper electrode in 0.1 M H2SO4 solution. *Mater. Chem. Phys.* **2010**, *121*, 354.

(24) Ohishi, Y.; Mukai, T.; Nagahara, M.; Yajima, M.; Kajikawa, N.; Miyahara, K.; Takano, T. Preparations of 5-alkylmethylidene-3-carboxymethylrhodanine derivatives and their aldose reductase inhibitory activity. *Chem. Pharm. Bull.* **1990**, *38*, 1911.

(25) Momose, Y.; Meguro, K.; Ikeda, H.; Hatanaka, C.; Oi, S.; Sohda, T. Studies on antidiabetic agents. X. Synthesis and biological activities

of pioglitazone and related compounds. *Chem. Pharm. Bull.* **1991**, *39*, 1440.
(26) Terashima, H.; Hama, K.; Yamamoto, R.; Tsuboshima, Kikkawa, M. R.; Hatanaka, I.; Shigeta, Y. J. Effects of a new aldose reductase inhibitor on various tissues in vitro. *J. Pharmacol. Exp. Ther.* **1984**, *229*, 226.
(27) Yoshioka, T.; Fujita, T.; Kanai, T.; Aizawa, Y.; Kurumada, T.; Hasegawa, K.; Horikoshi, H. Studies on hindered phenols and analogues. 1. Hypolipidemic and hypoglycemic agents with ability to inhibit lipid peroxidation. *J. Med. Chem.* **1989**, *32*, 421.
(28) Solmaz, R.; Şahin, E. A.; Döner, A.; Kardaş, G. The investigation of synergistic inhibition effect of rhodanine and iodide ion on the corrosion of copper in sulphuric acid solution. *Corros. Sci.* **2011**, *53*, 3231.
(29) Schweinsberg, D. P.; Bottle, S. E.; Otieno-Alego, V. A near-infrared FT-Raman (SERS) and electrochemical study of the synergistic effect of 1-[(1′,2′-dicarboxy)ethyl]-benzotriazole and KI on the dissolution of copper in aerated sulfuric acid. *J. Appl. Electrochem.* **1997**, *27*, 161.
(30) Abdel-Rahman, H. H.; Ahmed, A. M.; Harfoush, A. A.; Moustafa, A. H. E. The effect of aromatic and aliphatic amines on copper electrowinning from acidic sulphate electrolyte. *Hydrometallurgy* **2010**, *104*, 169.
(31) Amin, M. A. Role of dissolved oxygen reduction in improvement inhibition performance of ascorbic acid during copper corrosion in 0.50 mol/L sulphuric acid. *Chin. Chem. Lett.* **2010**, *21*, 341.
(32) Vaidyanathan, H.; Hackerman, N. Effect of furan derivatives on the anodic dissolution of Fe. *Corros. Sci.* **1971**, *11*, 737.
(33) Amin, M. A.; Khaled, K. F. Copper corrosion inhibition in O_2-saturated H_2SO_4 solutions. *Corros. Sci.* **2010**, *52*, 1194.
(34) Smyrl, W. H. Electrochemistry and corrosion on homogeneous and heterogeneous metal surface. In Bockris, J. O'M., Conway, B., Yager, E., White, R. E., Eds.; *Comprehensive Treatise of Electrochemistry*; Plenum Press: New York, London, 1981; Vol. *4*.
(35) Ma, H.; Chen, S.; Yin, B.; Zhao, S.; Liu, X. Impedance spectroscopic study of corrosion inhibition of copper by surfactants in the acidic solutions. *Corros. Sci.* **2003**, *45*, 867.
(36) Munoz, A.; Anton, J.; Guinon, J. L.; Herranz, V. P. Inhibition effect of chromate on the passivation and pitting corrosion of a duplex stainless steel in LiBr solutions using electrochemical techniques. *Corros. Sci.* **2007**, *49*, 3200.
(37) Behpour, M.; Ghoreishi, S. M.; Soltani Salavati-Niasari, N. M. The inhibitive effect of some bis-N, S-bidentate Schiff bases on corrosion behaviour of 304 stainless steel in hydrochloric acid solution. *Corros. Sci.* **2009**, *51*, 1073.
(38) Machnikova, E.; Whitmire, K.; Hackerman, H. N. Corrosion inhibition of carbon steel in hydrochloric acid by furan derivatives. *Electrochim. Acta* **2008**, *53*, 6024.
(39) Li, P.; Lin, J. Y.; Tan, K. L.; Lee, J. Y. Electrochemical impedance and X-ray photoelectron spectroscopic studies of the inhibition of mild steel corrosion in acids by cyclohexylamine. *Electrochim. Acta* **1997**, *42*, 605.
(40) Cheng, S. H.; Liu, T.; Chang, X.; Yin, Y. Carboxymethyl chitosan as an ecofriendly inhibitor for mild steel in 1 M HCl. *Mater. Lett.* **2007**, *61*, 3276.
(41) Khaled, K. F.; Babic-Samardzija, K.; Hackerman, N. Theoretical study of the structural effects of polymethylene amines on corrosion inhibition of iron in acid solutions. *Electrochim. Acta* **2005**, *50*, 2515.
(42) Ismail, K. M. Evaluation of cysteine as environmentally friendly corrosion inhibitor for copper in neutral and acidic chloride solutions. *Electrochim. Acta* **2007**, *52*, 7811.
(43) Ebenso, E. E.; Obot, I. B.; Murulana, L. C. Quinoline and its derivatives as effective corrosion inhibitors for mild steel in acidic medium. *Int. J. Electrochem. Sci.* **2010**, *5*, 1574.
(44) Migahed, M. A. Electrochemical investigation of the corrosion behaviour of mild steel in 2 M HCl solution in presence of 1-dodecyl-4-methoxy pyridinium bromide. *Mater. Chem. Phys.* **2005**, *93*, 48.
(45) Wang, X.; Yang, H.; Wang, F. An investigation of benzimidazole derivative as corrosion inhibitor for mild steel in different concentration HCl solutions. *Corros. Sci.* **2011**, *53*, 113.
(46) Küstü, C.; Emregül, K. C.; Atakol, O. Schiff bases of increasing complexity as mild steel corrosion inhibitors in 2 M HCl. *Corros. Sci.* **2007**, *49*, 2800.
(47) Tang, Y.; Yang, W.; Yin, X.; Liu, Y.; Wan, R.; Wang, J. Phenyl-substituted amino thiadiazoles as corrosion inhibitors for copper in 0.5 M H_2SO_4. *Mater. Chem. Phys.* **2009**, *116*, 479.
(48) Chao, C. Y.; Lin, L. F.; Macdonald, D. D. A point defect model for anodic passive films: I. Film growth kinetics. *J. Electrochem. Soc.* **1981**, *128*, 1187.
(49) Aruchamy, A.; Fujishima, A. Photoresponse of oxide layers on copper in aqueous electrolyte containing corrosion inhivitors. *J. Electroanal. Chem.* **1989**, *266*, 397.
(50) Ashassi-Sorkhabi, H.; Ghalebsaz-Jeddi, N.; Hashemzadeh, F.; Jahani, H. Corrosion inhibition of carbon steel in hydrochloric acid by some polyethylene glycols. *Electrochim. Acta* **2006**, *51*, 3848.
(51) Mattson, E.; Bockris, J. O'M. Galvanostatic studies of the kinetics of deposition and dissolution in the copper + copper sulphate system. *Trans. Faraday Soc.* **1959**, *55*, 1586.
(52) Moretti, G.; Guidi, F.; Grion, G. Tryptamine as a green iron corrosion inhibitor in 0.5 M deaerated sulphuric acid. *Corros. Sci.* **2004**, *46*, 387.
(53) Shaban, A.; Kalman, E.; Telegdi, J. An investigation of copper corrosion inhibition in chloride solutions by benzo-hydroxamic acids. *Electrochim. Acta* **1998**, *43*, 159.